Catalytic Cycle of Carbohydrate Dehydration by Lewis Acids: Structures and Rates from Synergism of Conventional and DNP NMR

Jensen, Pernille Rose; Meier, Sebastian

Published in:
Chemical Communications

Link to article, DOI:
10.1039/D0CC01756F

Publication date:
2020

Document Version
Peer reviewed version

ChemComm
Chemical Communications

Accepted Manuscript

This article can be cited before page numbers have been issued, to do this please use: P. Jensen and S. Meier, *Chem. Commun.*, 2020, DOI: 10.1039/D0CC01756F.

ROYAL SOCIETY OF CHEMISTRY

rsc.li/chemcomm

View Article Online
DOI: 10.1039/D0CC01756F

COMMUNICATION

Catalytic Cycle of Carbohydrate Dehydration by Lewis Acids: Structures and Rates from Synergism of Conventional and DNP NMR

Received 00th January 20xx,
Accepted 00th January 20xx

DOI: 10.1039/x0xx00000x

Pernille Rose Jensen[a] and Sebastian Meier*[b]

Lewis acids play key roles in many chemical reactions. Structural and functional (kinetic) detail in Lewis acid catalysed fructose conversion are derived herein by the combined use of conventional and dissolution dynamic nuclear polarization (D-DNP) NMR. Structural information obtained with D-DNP NMR was used to identify conditions that stabilize an elusive initial intermediate and to determine its chemical structure. Carbohydrate dehydration through this intermediate had been predicted computationally. Complementary kinetic NMR assays yielded rate constants spanning three orders of magnitude for the three biggest energy barriers in the catalytic cycle.

Lewis acidic metals catalyse many central chemical reactions,[1] including hydride shift, aldol, retro-aldol, Michael and retro-Michael reactions in the conversion of carbohydrates.[2-4] However, conversion pathways especially in carbohydrate dehydration are still debated controversially.[5] Increased insights into the reaction steps could simplify the improvement of Lewis acid catalysis, but most routine methods either lack the time resolution, sensitivity or chemical detail to support such insight. Accordingly, tracing conversion pathways, especially their fast and irreversible reactions, has remained a daunting task.[6]

In situ NMR spectroscopy has often been the method of choice for retrieving structural information and concentrations in ongoing organic reactions.[6-10] A particular stronghold of NMR spectroscopy is the ability to resolve equilibria of isomeric forms, for instance in carbohydrate substrates. Many of the relevant reactions converting carbohydrates occur by coordination of the low populated acyclic carbohydrate form to the catalyst. Moderate sensitivity and time resolution therefore aggravate molecular studies of the initial steps of catalytic carbohydrate conversion by conventional NMR spectroscopy. Considering these problems, the use of enhanced NMR methods should improve the discovery of the formation and conversion of intermediates in the Lewis acid catalysed reaction cycle. Specifically, dissolution dynamic nuclear polarization for enhancing NMR signals (D-DNP-NMR)[11] has shown promise in detecting previously elusive states in bio- and chemocalytic carbohydrate conversion.[12-15] This approach generates substrates with hyperpolarized nuclear spins and triggers reactions by rapid injection of the hyperpolarized substrate to a chemical or biological catalyst, while providing a signal increase by DNP on the order of 10 000.[16-18] Synergistic applications of D-DNP and conventional NMR techniques to characterize catalytic cycles on complementary time scales have remained very rare, however.[13, 19]

The current work aims to extend the mechanistic and kinetic understanding of carbohydrate dehydration pathways. D-DNP NMR was employed to detect transient early intermediates in the Lewis acid catalysed conversion of fructose. The fine structure of the transient signal was used to obtain insight into the structural motif that is initially formed in the reaction. This information was used to optimize the detection of the species in a temporarily stabilized sample using conventional NMR spectroscopy (Scheme 1). In this manner, a structural assignment of the transient intermediate could be achieved.

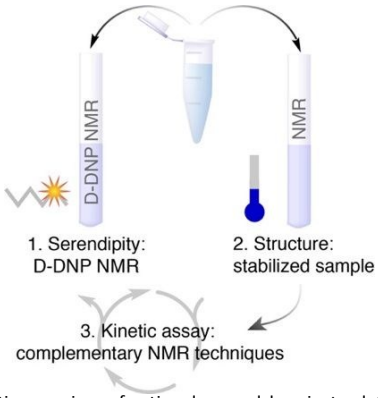

Scheme 1. Schematic overview of rationales used herein to detect an elusive intermediate, either through sample stabilization at low temperature or through the use of hyperpolarized substrate, and to trace NMR detectable intermediates in the catalytic cycle.

[a] *Department of Health Technology, Technical University of Denmark Elektrovej 349, 2800 Kgs. Lyngby, Denmark*
[b] *Department of Chemistry, Technical University of Denmark, Kemitorvet, Bulding 207, 2800 Kgs Lyngby (Denmark), E-mail: semei@kemi.dtu.dk*
†Electronic Supplementary Information (ESI) available: See DOI: 10.1039/x0xx00000x

View Article Online
DOI: 10.1039/D0CC01756F

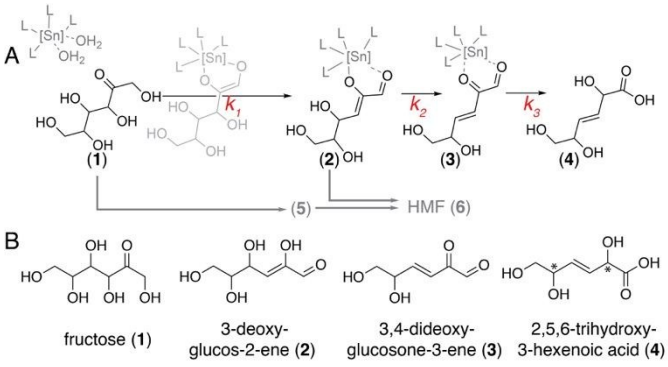

Scheme 2. Schematic overview of the mechanism (A) and NMR-detectable species (B) in the conversion of fructose (**1**) to THA (**4**). Competing acyclic and cyclic pathways (the latter via (4S,5R)-4-hydroxy-5-hydroxymethyl-4,5-dihydrofuran-2-carbaldehyde (**5**) to HMF, see Scheme S1 for details) are indicated in (A). THA is formed as diastereomeric compounds (asterisks indicate chiral centers in the product) from compounds with planar C2 stucture (B).

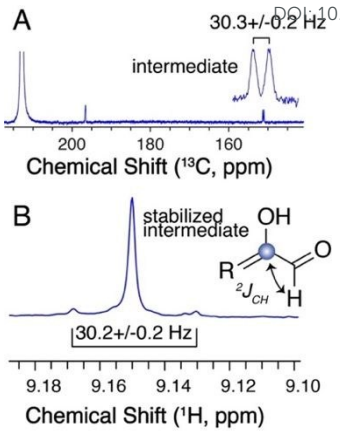

Figure 1. Detection of an enolic group adjacent to an aldehyde group through the $^{2}J_{CH}$ splitting of the ^{13}C enol signal in D-DNP ^{13}C NMR (A) and though the same splitting of the ^{1}H aldehyde signal in conventional ^{1}H NMR (B).

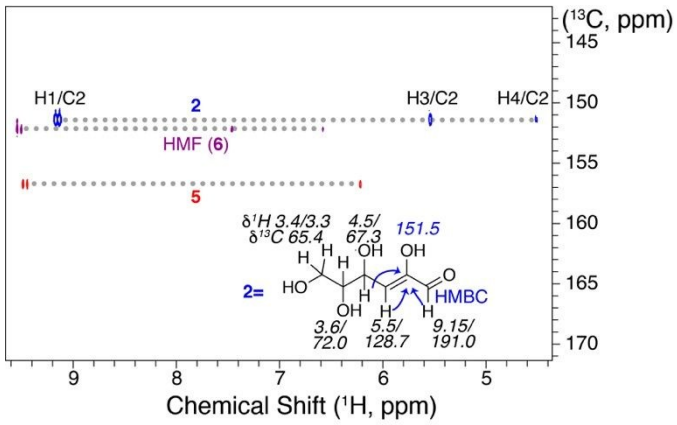

Figure 2. ^{1}H-^{13}C HMBC spectrum and chemical shift assignment for the structure determination of compound **2**. Minor species from the cyclic pathway to HMF (Scheme 2) are indicated.[8] The full spectrum is shown in Figure S4.

The finding experimentally validates that the lowest energy reaction pathway encompasses 3-deoxyglucos-2-ene (3-DGE, Scheme 2) as an on-pathway intermediate. Dehydration through this pathway intermediate had recently been predicted using machine learning based reaction sampling of carbohydrate dehydration.[5] Subsequently, time resolved D-DNP and conventional NMR spectra were combined in a first experimental determination of three catalytic rate constants in the catalytic cycle converting fructose to a prospective polymer building block.[20-23]

Experiments employing hyperpolarized [2-^{13}C] fructose and a rapid injection setup[9, 24, 25] were used in order to attempt detecting transient species that were formed immediately after mixing the substrate and the catalyst. The experiments indicated the formation of an enolic species with a characteristic ^{13}C chemical shift[26] of 151.5 ppm for the hydroxyl-bearing C2 in the double bond.[23] This serendipitous observation encouraged attempts to determine the structure of the intermediate and of obtaining sufficiently good time resolved data to determine the kinetics in the catalytic cycle (Scheme 1). This enol signal was split into a doublet by a scalar coupling of 30.3±0.3 Hz (Figure 1A). Coupling constants of 30 Hz to an enolic carbon, in turn, are characteristic for two-bond couplings to the proton in an adjacent aldehyde group. Having established the likely presence of an aldehyde proton coupling through a $^{2}J_{CH}$=30.3 Hz to the C2 in an enol group, it was possible to screen conventional ^{1}H NMR spectra for conditions, under which corresponding aldehyde signals emerge. This approach was assisted by the addition of 10% [2-^{13}C] fructose substrate in order to tenfold enhance the ^{1}H NMR satellite signals (each ~5% of the centre signal), which split with $^{2}J_{CH}$ = 30.2±0.2 Hz (Figure 1B). Reactions that were initiated for 30 seconds at 70 °C, rapidly cooled on ice and analysed at between -20 °C and +10 °C proved to permit the detection by conventional NMR of the intermediate compound **2**, which was stable on the minutes time scale at 10 °C (Figure S1).

Under conditions where the initial intermediate could be temporarily stabilized, ^{1}H-^{13}C HMBC (Figure 2) and ^{1}H-^{1}H TOCSY (Figure S2, S3) spectra were acquired to obtain structural assignments. The ^{1}H-^{13}C HMBC spectra benefitted from the knowledge of the scalar coupling between the aldehyde ^{1}H1 and the ^{13}C2 in order to maximize the detected signal (Figure 2). The ^{1}H-^{13}C HMBC spectra further profited from the use of non-uniform sampling of the indirect dimension in order to rapidly collect data on the temporarily stabilized intermediate. This approach validated that the aldehyde group detected in the spectrum shown in Figure 1B indeed is adjacent to the enol group detected in the spectrum shown in Figure 1A, as evidenced by the cross signal between the ^{1}H1 and the ^{13}C2 signal in the intermediate. Full chemical shift assignment and structure determination of the intermediate were subsequently achieved by a combination of assignment spectra (Figure 2, inset). The determination of the covalent structure for this previously postulated[4, 23, 27, 28] intermediate 3-DGE (**2**) complements the detection of the main reaction intermediate *trans*-3,4-DGE (**3**),[23] which is converted to THA (**4**), the recently discovered product of the cycle and a prospective polymer building block (Scheme 2; chemical shift assignments for **2**-**4** are given in Figure S5). The observation of 3-DGE rationalizes the previous detection of its keto tautomer 3-deoxyglucosone (3-DG) in reaction mixtures of Sn^{IV}-catalysed fructose

conversion,[4,23] as the on-pathway intermediate 3-DGE can tautomerise to 3-DG upon dissociation from the catalyst (Figure S3 and S4). Other Lewis acids than Sn^{IV} had proven less active in catalysing the acyclic pathway of carbohydrate conversion.[23]

D-DNP and conventional NMR are useful for kinetic assays on different time scales. Hyperpolarized signal fades on the seconds to minutes time scale and D-DNP NMR is best suited for the detection of fast reactions amongst multi-step transformations. Kinetic experiments were thus conducted under identical reaction conditions in order to quantify reaction rate constants by the complementary use of conventional NMR, thermal NMR, and computational modelling (Scheme 3). The real-time experiments are displayed in Figure 3. While conventional NMR captured the late intermediate and product signals, D-DNP NMR with optimized fructose polarization and sample delivery to the reaction mixture was successful in quantifying signal from the initial intermediate in a time-resolved manner with one second time resolution (Figure 4). Corresponding signals for the molecular species of Scheme 3 were integrated. Integrals for assays conducted on both time scales were separately fitted to models for the conversion of fructose to THA upon sequential elimination of the hydroxyl-groups at the 3- and 4-positions. Kinetic data and their fits to the model of Scheme 3 are displayed in Figure 4. Data were well described by a simple model of the reaction cycle encompassing sequential, irreversible elementary steps with **2** as an on-pathway intermediate (detailed accounts of the fitted models are given in the Supporting Information). Conventional NMR assays were suitable for determining an apparent kinetic rate constant for the conversion of **1** to **3** and for the reaction step converting intermediate **3** to **4**. D-DNP NMR resolved the two kinetics steps converting **1** to **3** by successive elimination of the 3- and 4-hydroxyl groups. Notably, excellent kinetic data could be obtained from single D-DNP NMR transients, although signals of **2** and **3** accumulate to less than 0.05% of the substrate signal in the D-DNP NMR assay owing to the slow initial reaction.

As a proof of concept, conventional and D-DNP NMR assays could be shown to return nearly identical values for the rate constant of substrate dehydration (k_{1app} = 0.00017 ± 0.00002 s^{-1} and k_1 = 0.00018 ± 0.00001 s^{-1}, respectively). Rate constants in the catalytic cycle were thus k_1 = 0.00018 s^{-1}, k_2 = 0.20(±0.02) and k_3 = 0.0016(±0.0002) s^{-1} (Figure 4, Scheme 4). Thus, rate constants differing by three orders of magnitude were derived. Replication indicated that the fitted values could be precisely determined. The initial conversion of fructose with k_{1app} has previously been described to encounter an activation energy of 107.2 kJ/mol.[23] Using the rate constants k_2 and k_3 and assuming comparable pre-exponential factors in transition state theory, the subsequent energy barriers can be estimated to 87.5 kJ/mol and 100.6 kJ/mol, respectively. Kinetic models of D-DNP NMR data also account for the general fading of hyperpolarization through pulsed excitation and T_1 relaxation (see Supporting Information for the kinetic expressions).[29, 30] Fitted T_1 values for

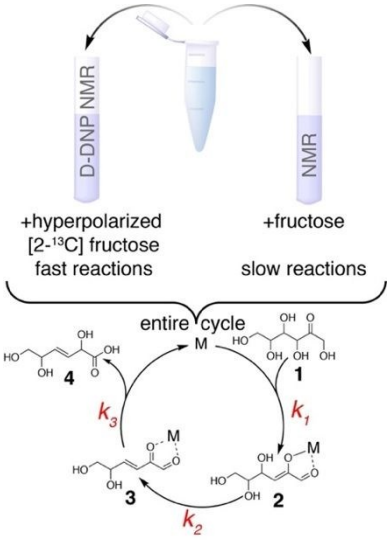

Scheme 3. Complementary real-time experiments (top) for determining three rate constants as displayed in the catalytic cycle (bottom).

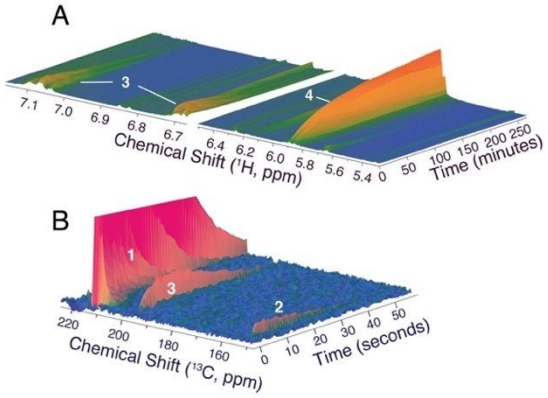

Figure 3. Real-time experiments using (A) conventional ^{1}H NMR with fructose substrate and (B) D-DNP NMR using hyperpolarized [2-^{13}C] fructose substrate to trace conversions using the C2 position as a molecular probe. Reaction conditions: 0.02g/ml $SnCl_4 \cdot 5H_2O$, 70 °C, d_6-DMSO/D_2O=85/15 (v/v).

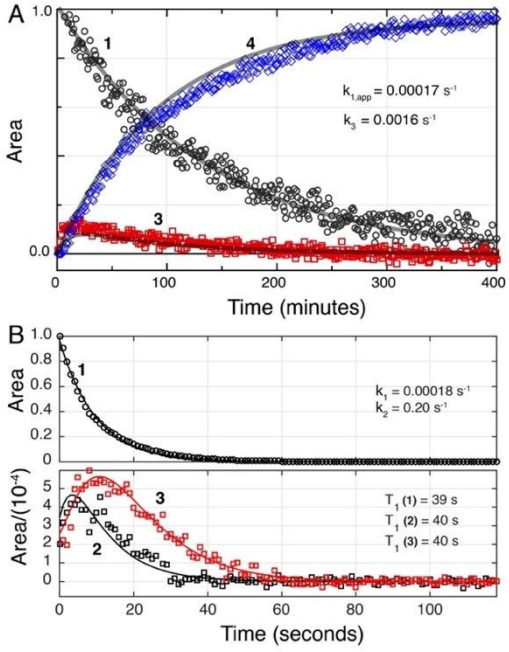

Figure 4. Integrals for the experiments shown in Figure 3. Fits to the kinetic model of Scheme 3 are shown for (A) conventional and (B) D-DNP NMR experiments. Rate constants and relaxation times for the fading of hyperpolarization are displayed.

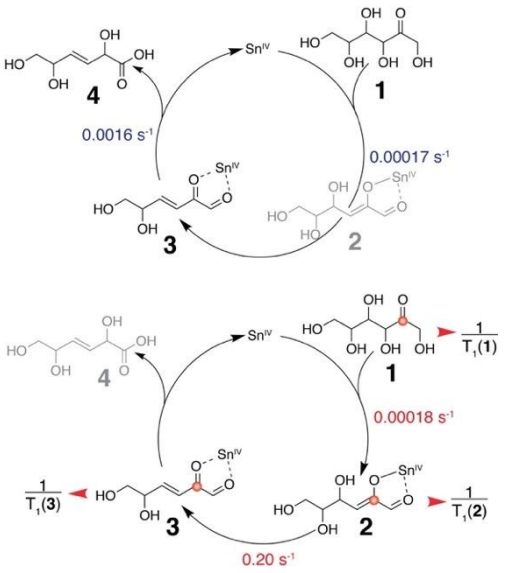

Scheme 4. Schematic overview of rate constants determined through conventional (top) and D-DNP (bottom) NMR.

the quaternary C2 carbon in compounds **1** to **3** were realistic (~40 s) at the assay temperature of 70 °C (Figure 4B).

In conclusion, an initial dehydrated intermediate was detected with D-DNP NMR, and spectral information was used to screen for conditions that allowed the structure of the previously postulated intermediate in the catalytic cycle to be determined as 3-deoxyglucos-2-ene. To this end, scalar coupling constant information retrieved from the D-DNP experiment was applied to a temporarily stabilized sample (10 °C). The structure determination validates recent computational predictions of a carbohydrate dehydration pathway through the enol tautomer of 3-deoxyglucosone.[5] Combined use of D-DNP and conventional NMR under relevant reaction conditions (70 °C) yielded insight into the rate constants (differing by three orders of magnitude) and thus into the three main energetic barriers (differing by 20 kJ/mol) of the catalytic cycle. Consistency with independent, simulated representations of the pathway,[5] gives reason to believe that the experimental data derived herein can play a role in the energetic understanding and optimization of Lewis acid catalysed carbohydrate conversion. Overall, conventional and D-DNP NMR were combined in a systematic and synergistic manner to experimentally observe elusive structural and kinetic details in the only recently described[4,23] acyclic conversion of C6 carbohydrates (see ESI† for experimental details).

Financial support from the Danish National Research Foundation (case number 124) and the Innovation Fund Denmark (case number 5150-00023B) is gratefully acknowledged. All 800 MHz NMR spectra were recorded on the spectrometer of the NMR Center DTU supported by the Villum Foundation.

Conflicts of interest

There are no conflicts to declare.

References

View Article Online
DOI: 10.1039/D0CC01756F

1 T. Gatzenmeier, M. van Gemmeren, Y. Xie, D. Höfler, M. Leutzsch and B. List, *Science*, 2016, **351**, 949.
2 M. S. Holm, S. Saravanamurugan and E. Taarning, *Science*, 2010, **328**, 602.
3 Y. Roman-Leshkov, M. Moliner, J. A. Labinger and M. E. Davis, *Angew. Chem. Int. Ed.*, 2010, **49**, 8954-8957.
4 S. Tolborg, S. Meier, I. Sádaba, S. G. Elliot, S. K. Kristensen, S. Saravanamurugan, A. Riisager, P. Fristrup, T. Skrydstrup and E. Taarning, *Green Chem.*, 2016, **18**, 3360-3369.
5 P.-L. Kang, C. Shang and Z.-P. Liu, *J. Am. Chem. Soc*, 2019, **141**, 20525-20536.
6 G. E. Wagner, S. Tassoti, S. Glanzer, E. Stadler, R. Herges, G. Gescheidt and K. Zangger, *Chem. Comm.*, 2019, **55**, 12575-12578.
7 M. H. Haindl, J. Hioe and R. M. Gschwind, *J. Am. Chem. Soc*, 2015, **137**, 12835-12842.
8 G. R. Akien, L. Qi and I. T. Horváth, *Chem. Comm.*, 2012, **48**, 5850-5852.
9 S. E. Denmark, B. J. Williams, B. M. Eklov, S. M. Pham and G. L. Beutner, *J. Org. Chem.*, 2010, **75**, 5558-5572.
10 D. A. Foley, J. Wang, B. Maranzano, M. T. Zell, B. L. Marquez, Y. Xiang and G. L. Reid, *Anal. Chem.*, 2013, **85**, 8928-8932.
11 J. H. Ardenkjaer-Larsen, B. Fridlund, A. Gram, G. Hansson, L. Hansson, M. H. Lerche, R. Servin, M. Thaning and K. Golman, *Proc. Natl. Acad. Sci. U. S. A.*, 2003, **100**, 10158-10163.
12 S. Meier, P. R. Jensen and J. O. Duus, *FEBS Lett.*, 2011, **585**, 3133-3138.
13 S. Meier, M. Karlsson and P. R. Jensen, *ACS Sustain. Chem. Eng.*, 2017, **5**, 5571-5577.
14 S. Meier, M. Karlsson, P. R. Jensen, M. H. Lerche and J. O. Duus, *Mol. Biosyst.*, 2011, **7**, 2834-2836.
15 K. R. Keshari, D. M. Wilson, A. P. Chen, R. Bok, P. E. Z. Larson, S. Hu, M. V. Criekinge, J. M. Macdonald, D. B. Vigneron and J. Kurhanewicz, *J. Am. Chem. Soc.*, 2009, **131**, 17591-17596.
16 M. Karlsson, P. R. Jensen, J. Ø. Duus, S. Meier and M. H. Lerche, *Appl. Magn. Reson.*, 2012, **43**, 223-236.
17 S. Bowen and C. Hilty, *Angew. Chem. Int. Ed.*, 2008, **47**, 5235-5237.
18 Y. Lee, G. S. Heo, H. Zeng, K. L. Wooley and C. Hilty, *J. Am. Chem. Soc.*, 2013, **135**, 4636-4639.
19 C. Yang, C. Harrison, E. S. Jin, D. T. Chuang, A. D. Sherry, C. R. Malloy, M. E. Merritt and R. J. DeBerardinis, *J. Biol. Chem.*, 2014, **289**, 6212-6224.
20 R. De Clercq, M. Dusselier, C. Christiaens, J. Dijkmans, R. I. Iacobescu, Y. Pontikes and B. F. Sels, *ACS Catal.*, 2015, **5**, 5803-5811.
21 R. De Clercq, M. Dusselier and B. F. Sels, *Green Chem.*, 2017, **19**, 5012-5040.
22 S. G. Elliot, C. Andersen, S. Tolborg, S. Meier, I. Sádaba, A. E. Daugaard and E. Taarning, *RSC Adv.*, 2017, **7**, 985-996.
23 E. Taarning, I. Sádaba, P. R. Jensen and S. Meier, *ChemSusChem*, 2019, **12**, 5086-5091.
24 J. F. McGarrity, J. Prodolliet and T. Smyth, *Org. Magn. Reson.*, 1981, **17**, 59-65.
25 K. H. Mok, T. Nagashima, I. J. Day, J. A. Jones, C. J. V. Jones, C. M. Dobson and P. J. Hore, *J. Am. Chem. Soc*, 2003, **125**, 12484-12492.
26 N. A. Keiko, N. V. Vchislo, E. A. Verochkina, Y. A. Chuvashev and L. I. Larina, *Mendeleev Commun.*, 2016, **26**, 431-433.
27 M. L. Wolfrom, R. D. Schuetz and L. F. Cavalieri, *J. Am. Chem. Soc.*, 1948, 70, 514-517.
28 M. J. Antal, W. S. L. Mok and G. N. Richards, *Carbohydr. Res.*, 1990, **199**, 91-109.
29 K. R. Keshari and D. M. Wilson, *Chem. Soc. Rev.*, 2014, **43**, 1627-1659.

30 G. Pagès and P. W. Kuchel, *Magn. Reson. Insights*, 2013, **6**, MRI.S11084.

View Article Online
DOI: 10.1039/D0CC01756F